Applications of the generalized gamma function to a fractional-order biological system

A.E. Matouk [a,b,*]

[a] *Department of Mathematics, College of Science Al-Zulfi, Majmaah University, Al-Majmaah, 11952, Saudi Arabia*
[b] *College of Engineering, Majmaah University, Al-Majmaah, 11952, Saudi Arabia*

ARTICLE INFO

ABSTRACT

In this work, variety of complex dynamics are found in a fractional-order antimicrobial resistance (AMR) model based on the generalized Gamma function. Firstly, the extended left and right Caputo fractional differential operators, respectively, ELCFDO and ERCFDO are introduced. The basic features of the ELCFDO are outlined. The ELCFDO is shown to have a new fractional parameter that affects the occurrence of the complex dynamics in the fractional AMR system. Secondly, discretization of the ELCFDO is studied using piecewise constant arguments. Then, complex dynamics of the discretized version of the fractional AMR system involving the ELCFDO are investigated such as the existence of Neimark–Sacker (NS) and flip bifurcations, the existence of closed invariant curves (CIC), the existence of strange attractors with fractal or multi-fractal structures, and chaotic attractors. Finally, an extension of the fractal-fractional operator (FFO) that combines fractal and fractional differentiation is carried out based on the generalized Gamma function. The extended FFO (EFFO) is applied to the proposed AMR system, which also generates similar complex dynamics.

1. Introduction

The mathematical modeling provides essential and precise tools to describe and understand the complex behaviors in some real-world problems through the simulations of these problems in the form of differential equations that can have ordinary derivatives [1–3], partial derivatives [4,5], or fractional derivatives [6,7]. On the other hand, the study of real-world nonlinear problems through fractals has become a focal topic for research [8].

In fact, the investigations of the mathematical properties of fractional derivatives give rise to the so-called fractional calculus (FC) which has received increasing interest by engineers, scientists and economists, who become able to make more realistic descriptions and precise analyses for their related real-world problems using the aid of FC [9–17]. The high importance of the FC in mathematical modeling is due to its highest adequacy for measuring the natural phenomena. In addition, the biological models that are described in terms of FC involve the memory effect, which is considered to be a powerful tool in modeling the epidemiological diseases and viral dynamics. For example, Padder et al. studied the generalized tumor model using the Caputo fractional differential operator (CFDO) [18]. In Ref. [19], Qureshi and Memon analyzed a model of measles disease using the Caputo-Fabrizio-Caputo derivatives. In Ref. [20], Jan et al. investigated a model for the human immunodeficiency virus using the CFDO.

Indeed, the CFDO is considered to be a vital tool for modeling many scientific and engineering phenomena because its related initial

---

values can easily be determined [21]. Consequently, the CFDO is widely used in real-world applications. Obviously, the fractional operator has one order represented by the.

fractional order (parameter). On the other hand, the concept of fractal-fractional operators (FFOs) has been introduced in Ref. [22]. The FFO is shown to have two orders; the fractal dimension in addition to the fractional parameter. Hence, the FFO can better explain the hereditary properties and memory effects of some ecological, financial and physical models. One of the most familiar FFOs is the Atangana-Baleanu FFO in the Caputo sense (FFO-ABC), which consists of a Mittag-Leffler function. Another famous type of the FFOs has a power law-type kernel and is known as the fractal-fractional operator in the Caputo sense (FFO–C).

The discovery of the Gamma function dates back to the 18th century. It is considered to be one of the most interesting special functions, which has useful applications in statistics, physics and engineering. A generalization (or an extension) of the gamma function was introduced in Ref. [23] that has promising applications to interdisciplinary fields, such as, mathematical physics, mathematical modeling, engineering and analytical number theory. Actually, both the CFDO and FFO-C depend on the Euler Gamma function. So, inserting the extended Gamma function in these fractional operators will lead to demonstrating a variety of rich dynamical behaviors in the mathematical model. In addition, the extended operators will provide higher adequacy and better estimation of the natural phenomena.

Recently, the recurrence of some diseases which were thought to have disappeared has been discovered. Antimicrobial resistance and multi-drug resistance are considered to be among the possible reasons for such observations. In Ref. [24], Ahmed and Matouk introduced a simple antimicrobial resistance model, or simply the AMR model, that can be used to describe the competition between susceptible and resistant species. The dynamics of the fractional AMR system on complex networks have also been discussed in Ref. [24], where the classic CFDO was used.

Here, we intend to investigate the complex dynamics of the AMR system involving the ELCFDO and the extended FFO-C (EFFO-C). To summarize the advantages of the AMR model based on the generalized Gamma function, we first draw attention to the fact that the new fractional operators have more degrees of freedom than the classic fractional ones, which enable the AMR system to display more complex dynamics compared with other AMR models involving the classic operators. In addition, the motivations of this work are clearly provided by comparing the results obtained via the new fractional operators with the results obtained via the classic fractional operators. The outcome of this comparison confirms that the proposed new fractional operators are better candidates to handle the complex dynamics in the AMR models. Then, we study the discretization of the ELCFDO with piecewise constant arguments in the AMR model since the transmitted data on diseases are typically discrete. Furthermore, the discrete AMR model enables us to obtain rich complex behaviors in contrast to its continuous-time form. Moreover, the discrete AMR model enables us to obtain its solutions in terms of a finite representation of elementary functions, unlike its continuous-time counterpart which often has unknown precise analytical solutions. The discrete-time AMR system is shown to exhibit NS and flip bifurcations, CIC, chaotic attractors and coexistence of multi-strange attractors.

The structure of the rest of this work is outlined as follows; In Section 2, the ELCFDO and ERCFDO are introduced based on the generalized Gamma function. The related fractional integrals are also presented. The mathematical analyses of the new derivatives are clearly derived and rigorously proved in this Section. Furthermore, the FFO-C is modified based on the generalized Gamma function. In Section 3, the mathematical equations of the AMR model are presented in integer- and fractional-order forms. In addition, the discretization of the AMR system involving the ELCFDO are studied using piecewise constant arguments. Complex dynamics in the AMR system involving the ELCFDO are investigated in Section 4. The rich complex dynamical behaviors of the fore mentioned discretized AMR system are illustrated in Section 5. The complex dynamics of the AMR system involving the EFFO-C are investigated in Section 6. In Section 7, the concluding statements and the discussion points about this work are summarized.

2. Fundamental concepts of fractional calculus

The ELCFDO is described by Eq. (1)

$$
{}^{E}_{C}\mathrm{O}^{q,\eta}_{a+}\varpi(t) = {}^{E}_{RL}\mathrm{I}^{l-q,\eta}_{a+}\frac{d^{l}\varpi(t)}{dt^{l}}, q > 0, \tag{1}
$$

where $l = \lceil q \rceil$ and ${}^{E}_{RL}\mathrm{I}^{\xi,\eta}_{a+}\varphi(t) = [\int\limits_{a}^{t}(t-x)^{\xi-1}\varphi(x)dx]/\Gamma_{Ext.}(\xi,\eta), \xi > 0, t > a,$ represents the ξ th-order extended left Riemann-Liouville

(ELRL) fractional integral, and $\Gamma_{Ext.}(.)$ is the generalized Gamma function defined by

$$
\Gamma_{Ext.}(\xi,\eta) = \int\limits_{0}^{+\infty}\frac{y^{\xi-1}}{e^{\eta y}}dy, \xi, \eta > 0.
$$

Notations: The superscript "T" represents the transpose of the matrix. By the abbreviation 'IVP', we mean the initial value problem. By $N, Z^{+}, R, C,$ we refer to the sets of all natural numbers, positive integers, real numbers and complex numbers, respectively. The number j is $\sqrt{-1}$. The number e is the Euler's number. The notation "Re" refers to the real part of the number. $L^{1}([a,b])$ (for simplicity L^{1}) is the set of Lebesgue integrable functions on $[a,b]$. The set of all continuous functions on $[a,b], a, b \in R$ is represented by $C([a,b])$. The set of all absolutely continuous functions on $[a,b]$ is represented by $AC([a,b])$. The set of $m-$ times differentiable functions such that the m-th derivatives are continuous on $[a,b]$ is represented by $C^{m}([a,b])$. $\Gamma(.)$ is the Euler Gamma function. $B(.,.)$ is the Beta function.

The operation $\langle .,. \rangle$ refers to the standard scalar product in R^n. The Euclidean norm is denoted by $\|.\|$. The floor function is denoted by $[.]$. By $ceil(q)$, we mean the ceiling function of q, or simply $\lceil q \rceil$..

Now, the classic CFDO is presented as (See Eq. (2))

$$_C O_{a+}^q \varpi(t) = \eta^{q-l}\, _C^E O_{a+}^{q,\eta} \varpi(t). \tag{2}$$

So, the classic left Riemann-Liouville (LRL) integral is defined by Eq. (3)

$$_{RL} I_{a+}^{\xi} \varphi(t) = \frac{1}{\eta^{\xi}}\, _{RL}^E I_{a+}^{\xi,\eta} \varphi(t). \tag{3}$$

The LRL integral satisfies the following theorem [25] and lemma [26].

Theorem 1. Suppose that $\varpi(t) \in L^1$ and $\varphi(t) \in L^1$. Then, the LRL operator satisfies the interpolation, the linearity and the commutative prosperities. i.e.

(i) $\lim_{\xi \to l} {}_{RL} I_{0+}^{\xi} \varpi(t) = {}_{RL} I_{0+}^{l} \varpi(t), l \in N$, where the LRL integral is the classical operator for $l-$ fold integration;

$$_{RL} I_{0+}^{\xi} [k_1 \varpi(t) + k_2 \varphi(t)] = k_1 {}_{RL} I_{0+}^{\xi} \varpi(t) + k_2 {}_{RL} I_{0+}^{\xi} \varphi(t), \forall k_1, k_2 \in C; \tag{4}$$

(iii) $\left({}_{RL} I_{0+}^{\xi_1} \right) \left({}_{RL} I_{0+}^{\xi_2} \varpi \right) (t) = \left({}_{RL} I_{0+}^{\xi_2,\eta} \right) \left({}_{RL} I_{0+}^{\xi_1} \varpi \right) (t)$, where $\xi_i \in \{0\} \cup R^+, i = 1, 2..$

Lemma 1. *If $\xi \in (0,1)$ and $\varpi \in C[0,b]$ then the LRL integral $\left. {}_{RL} I_{0+}^{\xi} \varpi(t) \right|_{t=0}$ vanishes.*

The ξ th-order extended right Riemann-Liouville (ERRL) fractional integral is

$$_{RL}^E I_{b-}^{\xi,\eta} \varphi(t) = \left[\int_t^b (x-t)^{\xi-1} \varphi(x)dx \right] \Big/ \Gamma_{Ext.}(\xi,\eta), \xi > 0, t < b.$$

Hence, the ERCFDO is given by.

$$_C^E O_{b-}^{q,\eta} \varpi(t) = {}_{RL}^E I_{b-}^{l-q,\eta} \left(-\frac{d}{dt} \right)^l \varpi(t), q > 0, l = ceil(q).$$

Furthermore, the ELCFDO and ERCFDO satisfy the following properties.

Lemma 2. (i) Let $c \neq 0$ be a constant real number then $_C^E O_{a+}^{q,\eta} c = {}_C^E O_{b-}^{q,\eta} c = 0..$

(ii) Let $\varpi(t) \in AC([a,b])$ and $q \in (0,1)$, then $\lim_{q \to 1} {}_C^E O_{a+}^{q,\eta} \varpi(t) = \frac{d\varpi(t)}{dt}..$

Proof. To prove part (i), we firstly rewrite the ELCFDO as follows

$$_C^E O_{a+}^{q,\eta} \varpi(t) = \frac{1}{\Gamma_{Ext.}(1-q,\eta)} \int_a^t (t-x)^{1-q-1} \varpi^{(1)}(x)dx.$$

where the $1-$ th derivative $\varpi^{(1)}(x) = 0$. So, the ELCFDO is integrated as

$$_C^E O_{a+}^{q,\eta} \varpi(t) = \frac{-1}{\Gamma_{Ext.}(1-q,\eta)} \left[\frac{(t-x)^{1-q}}{1-q} \right]_a^t \varpi^{(1)}(x) = \frac{1}{\Gamma_{Ext.}(1-q,\eta)} \left(\frac{(t-a)^{1-q}}{1-q} \right)(0) = 0.$$

Similarly, we can prove that $_C^E O_{b-}^{q,\eta} c = 0..$

To prove part (ii), we use integration by parts as follows

$$_C^E O_{a+}^{q,\eta} \varpi(t) = \frac{1}{\Gamma_{Ext.}(1-q,\eta)} \int_a^t (t-x)^{-q} \varpi^{(1)}(x)dx$$

$$= \frac{1}{\Gamma_{Ext.}(1-q,\eta)} \left(-\varpi^{(1)}(x) \frac{(t-x)^{1-q}}{1-q} \Big|_a^t + \int_a^t \varpi^{(2)}(x) \frac{(t-x)^{1-q}}{1-q}dx \right)$$

$$= \frac{\eta^{1-q}}{\Gamma(2-q)} \left(\varpi^{(1)}(a)(t-a)^{1-q} + \int_a^t \varpi^{(2)}(x)(t-x)^{1-q}dx \right).$$

Thus, $\lim_{q \to 1} {}_C^E O_{a+}^{q,\eta} \varpi(t) = (\varpi^{(1)}(a) + \varpi^{(1)}(x)\big|_a^t) = \frac{d\varpi(t)}{dt}. \square$

The following lemmas hold for the ELRL fractional integral.

Lemma 3. ${}^{E}_{RL}I^{1,\eta}_{a+}\varpi(t) = \eta \int_{a}^{t} \varpi(x)dx.$

Proof. ${}^{E}_{RL}I^{1,\eta}_{a+}\varpi(t) = [\int_{a}^{t} \varpi(x)dx]/\Gamma_{Ext.}(1,\eta) = \eta \int_{a}^{t} \varpi(x)dx..$

Lemma 4. The semi-group property is satisfied. i.e. If $\varpi(t) \in L^1$, then

$$\left({}^{E}_{RL}I^{\xi_1,\eta}_{0+}\right)\left({}^{E}_{RL}I^{\xi_2,\eta}_{0+}\varpi\right)(t) = \left({}^{E}_{RL}I^{\xi_1+\xi_2,\eta}_{0+}\varpi\right)(t).$$

Proof.

$$\left({}^{E}_{RL}I^{\xi_1,\eta}_{0+}\right)\left({}^{E}_{RL}I^{\xi_2,\eta}_{0+}\varpi\right)(t) = \frac{1}{\Gamma_{Ext.}(\xi_1,\eta)}\int_{0}^{t}(t-x)^{\xi_1-1}\left({}^{E}_{RL}I^{\xi_2,\eta}_{0+}\varpi\right)(x)dx.$$

$$= \frac{1}{\Gamma_{Ext.}(\xi_1,\eta)\Gamma_{Ext.}(\xi_2,\eta)}\int_{0}^{t}\int_{0}^{x}(t-x)^{\xi_1-1}(x-y)^{\xi_2-1}\varpi(y)dydx$$

$$= \frac{1}{\Gamma_{Ext.}(\xi_1,\eta)\Gamma_{Ext.}(\xi_2,\eta)}\int_{0}^{t}\varpi(y)\left(\int_{y}^{t}(t-x)^{\xi_1-1}(x-y)^{\xi_2-1}dx\right)dy.$$

Then, we use the change of variables $x = y + (t-y)\tau$, which yields

$$\left({}^{E}_{RL}I^{\xi_1,\eta}_{0+}\right)\left({}^{E}_{RL}I^{\xi_2,\eta}_{0+}\varpi\right)(t) = \frac{\eta^{\xi_1+\xi_2}}{\Gamma(\xi_1)\Gamma(\xi_2)}\int_{0}^{t}(t-y)^{\xi_1+\xi_2-1}\varpi(y)B(\xi_2,\xi_1)dy,$$

where

$$B(\xi_2,\xi_1) = \int_{0}^{1}(1-\tau)^{\xi_1-1}\tau^{\xi_2-1}d\tau = \frac{\Gamma(\xi_1)\Gamma(\xi_2)}{\Gamma(\xi_1+\xi_2)}.$$

hence,

$$\left({}^{E}_{RL}I^{\xi_1,\eta}_{0+}\right)\left({}^{E}_{RL}I^{\xi_2,\eta}_{0+}\varpi\right)(t) = \frac{\eta^{\xi_1+\xi_2}}{\Gamma(\xi_1+\xi_2)}\int_{0}^{t}(t-y)^{\xi_1+\xi_2-1}\varpi(y)dy$$

$$= \frac{1}{\Gamma_{Ext.}(\xi_1+\xi_2,\eta)}\int_{0}^{t}(t-y)^{\xi_1+\xi_2-1}\varpi(y)dy = \left({}^{E}_{RL}I^{\xi_1+\xi_2,\eta}_{0+}\varpi\right)(t).$$

□

Lemma 5. $\lim_{\xi\to l}{}^{E}_{RL}I^{\xi,\eta}_{0+}\varpi(t) = {}^{E}_{RL}I^{l,\eta}_{0+}\varpi(t)$ uniformly on $[0,b], l \in N$.

proof. According to part (i) of Theorem 1 and Eq. (3), the proof is straightforwardly obtained. □

Lemma 6. The ELRL fractional integral is a linear operator.

proof. Multiplying both sides of Eq. (4) by η^{ξ}, where $\eta > 0$, the proof is directly obtained. □

Lemma 7. $\left({}^{E}_{RL}I^{\xi_1,\eta}_{0+}\right)\left({}^{E}_{RL}I^{\xi_2,\eta}_{0+}\varpi\right)(t) = \left({}^{E}_{RL}I^{\xi_2,\eta}_{0+}\right)\left({}^{E}_{RL}I^{\xi_1,\eta}_{0+}\varpi\right)(t)$, where $\xi_i, i = 1,2$ are non-negative reals.

Proof. According to Eq. (3) and the linearity property of the LRL operator, we get

$$\left({}^{E}_{RL}I^{\xi_1,\eta}_{0+}\right)\left({}^{E}_{RL}I^{\xi_2,\eta}_{0+}\varpi\right)(t) = \left(\eta^{\xi_1}{}_{RL}I^{\xi_1}_{0+}\right)\left(\eta^{\xi_2}{}_{RL}I^{\xi_2}_{0+}\varpi\right)(t) = \eta^{\xi_1+\xi_2}\left({}_{RL}I^{\xi_1}_{0+}\right)\left({}_{RL}I^{\xi_2}_{0+}\varpi\right)(t).$$

then, according to the commutative property of the LRL operator, the last relation is reduced to

$$\left({}^{E}_{RL}I^{\xi_1,\eta}_{0+}\right)\left({}^{E}_{RL}I^{\xi_2,\eta}_{0+}\varpi\right)(t) = \eta^{\xi_1+\xi_2}\left({}_{RL}I^{\xi_2}_{0+}\right)\left({}_{RL}I^{\xi_1}_{0+}\varpi\right)(t).$$

Again using the linearity property, we get

$$\left({}^{E}_{RL}I^{\xi_1,\eta}_{0+}\right)\left({}^{E}_{RL}I^{\xi_2,\eta}_{0+}\varpi\right)(t) = \left(\eta^{\xi_2}{}_{RL}I^{\xi_2}_{0+}\right)\left(\eta^{\xi_1}{}_{RL}I^{\xi_1}_{0+}\varpi\right)(t).$$

Then, using Eq. (3), the proof is completed. □

Lemma 8. ${}^{E}_{RL}I^{\xi,\eta}_{0+}t^{\varepsilon} = \frac{\Gamma_{Ext.}(\varepsilon+1,\eta)}{\Gamma_{Ext.}(\varepsilon+\xi+1,\eta)}t^{\xi+\varepsilon}$ for $\varepsilon + 1 > 0$.

Proof. The LHS is written as

$$
{}^{E}_{RL}I^{\xi,\eta}_{0+}t^{\varepsilon} = \left[\int_{0}^{t} (t-x)^{\xi-1}x^{\varepsilon}dx \right] \bigg/ \Gamma_{Ext.}(\xi,\eta).
$$

Let $y = x/t, \varepsilon + 1 > 0,$ then

$$
{}^{E}_{RL}I^{\xi,\eta}_{0+}t^{\varepsilon} = t^{\xi+\varepsilon}\left[\int_{0}^{1} (1-y)^{\xi-1}y^{\varepsilon}dy \right] \bigg/ \Gamma_{Ext.}(\xi,\eta) = \frac{t^{\xi+\varepsilon}}{\Gamma_{Ext.}(\xi,\eta)}B(\varepsilon+1,\xi) = \frac{\Gamma(\varepsilon+1)\Gamma(\xi)}{\Gamma_{Ext.}(\xi,\eta)\Gamma(\varepsilon+\xi+1)}t^{\xi+\varepsilon}.
$$

Now, since $\Gamma(\xi) = \eta^{\xi}\Gamma_{Ext.}(\xi,\eta),$ we obtain

$${}^{E}_{RL}I^{\xi,\eta}_{0+}t^{\varepsilon} = \frac{[\eta^{1+\varepsilon}\Gamma_{Ext.}(\varepsilon+1,\eta)][\eta^{\xi}\Gamma_{Ext.}(\xi,\eta)]}{\Gamma_{Ext.}(\xi,\eta)[\eta^{\varepsilon+\xi+1}\Gamma_{Ext.}(\varepsilon+\xi+1,\eta)]}t^{\xi+\varepsilon} = \frac{\Gamma_{Ext.}(\varepsilon+1,\eta)}{\Gamma_{Ext.}(\varepsilon+\xi+1,\eta)}t^{\xi+\varepsilon}. \quad \square$$

Lemma 9. *Let $\xi \in (0,1)$; if $\varpi \in C[0,b]$ then the quantity $\left. {}^{E}_{RL}I^{\xi,\eta}_{0+}\varpi(t) \right|_{t=0}$ vanishes.*

Proof. According to Eq. (3), we obtain

$$
\left. {}^{E}_{RL}I^{\xi,\eta}_{0+}\varpi(t) \right|_{t=0} = \eta^{\xi} {}_{RL}I^{\xi}_{0+}\varpi(t)\bigg|_{t=0},
$$

where $\eta > 0$. Then, based on Lemma 1, the quantity in the RHS is vanished. $\square$

Lemma 10. ${}^{E}_{RL}I^{\xi,\eta}_{a+}\varpi(t) = \frac{c}{\xi\Gamma_{Ext.}(\xi,\eta)}(t-a)^{\xi}$, whenever $\varpi(t) = c$ is a constant function.

Proof. Let $\varpi(t) = c$ be a constant function, then based on the definition of the ELRL fractional integral, we get

$$
{}^{E}_{RL}I^{\xi,\eta}_{a+}c = \frac{c}{\Gamma_{Ext.}(\xi,\eta)}\int_{a}^{t}(t-x)^{\xi-1}dx = \frac{-c}{\xi\Gamma_{Ext.}(\xi,\eta)}\left[(t-x)^{\xi}\right]_{a}^{t} = \frac{-c}{\xi\Gamma_{Ext.}(\xi,\eta)}\left[0 - (t-a)^{\xi}\right]
$$

$$
= \frac{c}{\xi\Gamma_{Ext.}(\xi,\eta)}(t-a)^{\xi}.
$$

on the other hand, the EFFO-C is defined as

$$
{}^{EFF}_{C}O^{q,p,\eta}_{0,t}(\varpi(t)) = \frac{1}{\Gamma_{Ext.}(l-q,\eta)}\frac{d}{dt^{p}}\int_{0}^{t}\frac{\varpi(x)dx}{(t-x)^{1+q-l}}, \tag{5}
$$

where $p > 0$ represents the fractal-fractional parameter, $q > 0$ represents the order of the fractional derivative such that $q,p \in (l-1,l), l \in N$ and $\frac{d\varpi(t)}{dt^{p}} = \lim_{x \to t}\frac{\varpi(x)-\varpi(t)}{x^{p}-t^{p}}.$.

Obviously, both the ELCFDO and the ERCFDO have the memory effect and hereditary features that can be very suitable for modeling biological systems. In addition, the new extended fractional operators include all the dynamics of their classic fractional counterparts since they have higher degrees of freedom (such as the positive parameter η), which make them better candidates to handle the complex dynamics in biological models.

3. The biological system

The AMR system [20] is defined by Eq. (6) as follows:

$$
\begin{aligned}
\frac{dU}{dt} &= \alpha'U(1-U) - UV, \\
\frac{dV}{dt} &= \beta'UV - \gamma'V,
\end{aligned} \tag{6}
$$

where U and V represent susceptible species and resistant species, respectively. The model's positive parameters are mentioned in the parameter set $A' = \{\alpha',\beta',\gamma'\}$ and they have dimensions of 1/time. The system's equilibrium points are $P_0 = (0,0), P_1 = (1,0)$ and $P'_2 = (\gamma'/\beta',\alpha'(\beta'-\gamma')/\beta')$ provided that $\beta' > \gamma'$..

The fractional form of the AMR system (6) can be written in terms of the ELCFDO, as defined by Eq. (7), as follows

$$
\begin{aligned}
{}^{E}_{C}O^{q,\eta}_{0+}u(t) &= \alpha u(1-u) - uv, \\
{}^{E}_{C}O^{q,\eta}_{0+}v(t) &= \beta uv - \gamma v,
\end{aligned} \tag{7}
$$

in which the new state variables are redefined as $u = U^{(q)}, v = V^{(q)}$ that, respectively, refer to portion of susceptible species and resistant species. The initial conditions (ICs) of the AMR system (7) are described as

$$u(0) = u_0 \text{ and } v(0) = v_0.$$

Then, we define the new positive parameters α_0, β_0 and γ_0, whose dimensions are of 1/time. Thus, the new parameters of system (7) are defined as

$\alpha = \alpha_0^q, \beta = \beta_0^q$ and $\gamma = \gamma_0^q$, in which the dimensions are of $1/(time)^q$. Thus, system (7) has the parameter set $A = \{\alpha, \beta, \gamma\}$. The advantages of using the ELCFDO for the AMR model are summarized as; Firstly, the ELCFDO generalizes the classic Caputo operators that are widely used in real-world problems, and therefore the ELCFDO is more convenient for modeling real-world phenomena. Secondly, the hereditary features, memory effects, and higher degree of freedom that are captured by the ELCFDO enable the researchers to have a more precise description of the model's dynamical behaviors.

Then, we will apply a discretization method to system (7) with piecewise constant arguments in which the system is rewritten in Eq. (8) as

$$
\begin{aligned}
{}_C^E O_{0+}^{q,\eta} u(t) &= \alpha u([\lambda]m)(1 - u([\lambda]m)) - u([\lambda]m)v([\lambda]m), \\
{}_C^E O_{0+}^{q,\eta} v(t) &= \beta u([\lambda]m)v([\lambda]m) - \gamma v([\lambda]m).
\end{aligned}
\tag{8}
$$

where $\lambda = t/m$ and $m > 0$ represents the discretization parameter. Firstly, when $t \in [0, m)$, it follows that $0 \le \lambda < 1$ which implies that

$$
\begin{aligned}
{}_C^E O_{0+}^{q,\eta} u(t) &= \alpha u_0(1 - u_0) - u_0 v_0, \\
{}_C^E O_{0+}^{q,\eta} v(t) &= \beta u_0 v_0 - \gamma v_0.
\end{aligned}
\tag{9}
$$

System (9) has the solution given by Eq. (10) as follows

$$
\begin{aligned}
u_1(t) &= u_0 + {}_{RL}^E I_{0+}^{q,\eta}(\alpha u_0(1 - u_0) - u_0 v_0) = u_0 + \frac{t^q}{q\Gamma_{Ext.}(q,\eta)}(\alpha u_0(1 - u_0) - u_0 v_0), \\
v_1(t) &= v_0 + {}_{RL}^E I_{0+}^{q,\eta}(\beta u_0 v_0 - \gamma v_0) = v_0 + \frac{t^q}{q\Gamma_{Ext.}(q,\eta)}(\beta u_0 v_0 - \gamma v_0).
\end{aligned}
\tag{10}
$$

Secondly, we assume that $t \in [m, 2m)$, which implies that $1 \le \lambda < 2$. So, we obtain system (11)

$$
\begin{aligned}
{}_C^E O_{0+}^{q,\eta} u(t) &= \alpha u_1(1 - u_1) - u_1 v_1, \\
{}_C^E O_{0+}^{q,\eta} v(t) &= \beta u_1 v_1 - \gamma v_1,
\end{aligned}
\tag{11}
$$

which has the following solution

$$
u_2(t) = u_1(m) + {}_{RL}^E I_{m+}^{q,\eta}(\alpha u_1(m)(1 - u_1(m)) - u_1(m)v_1(m)) = u_1(m) + \frac{(t - m)^q}{q\Gamma_{Ext.}(q,\eta)}(\alpha u_1(m)(1 - u_1(m)) - u_1(m)v_1(m)),
$$

$$
v_2(t) = v_1(m) + {}_{RL}^E I_{m+}^{q,\eta}(\beta u_1(m)v_1(m) - \gamma v_1(m)) = v_1(m) + \frac{(t - m)^q}{q\Gamma_{Ext.}(q,\eta)}(\beta u_1(m)v_1(m) - \gamma v_1(m)).
$$

After n times, we obtain system (12)

$$
\begin{aligned}
u_{n+1}(t) &= u_n(nm) + \frac{(t - nm)^q}{q\Gamma_{Ext.}(q,\eta)}(\alpha u_n(nm)(1 - u_n(nm)) - u_n(nm)v_n(nm)), \\
v_{n+1}(t) &= v_n(nm) + \frac{(t - nm)^q}{q\Gamma_{Ext.}(q,\eta)}(\beta u_n(nm)v_n(nm) - \gamma v_n(nm)),
\end{aligned}
\tag{12}
$$

where $t \in [nm, (n+1)m)$. For $t \to (n+1)m$, system (12) can be formulated in terms of equation (13) as follows

$$
\begin{aligned}
u_{n+1} &= u_n + \mu(q, m, \eta)[\alpha u_n(1 - u_n) - u_n v_n], \\
v_{n+1} &= v_n + \mu(q, m, \eta)[\beta u_n v_n - \gamma v_n],
\end{aligned}
\tag{13}
$$

where $\mu(q, m, \eta) = \frac{m^q}{q\Gamma_{Ext.}(q,\eta)}$. The last system has the equilibrium solutions P_0, P_1 and $P_2 = (\gamma/\beta, \alpha(\beta - \gamma)/\beta)$.

4. Complex dynamics in the AMR system (7)

4.1. New PECE scheme for the numerical simulations of system (7)

To explain our numerical method which is based on the well-known PECE scheme [27], we introduce the following IVP

$$\begin{cases} {}_{C}^{E}O_{a+}^{q,\eta}\varpi(t) = w(t,\varpi(t)), t \in [a,T], \\ \varpi^{(r)}(a) = \varpi_0^{(r)}, r = 0,1,...,l-1, \end{cases} \tag{14}$$

where $l = ceil(q), q > 0, \eta > 0, a \geq 0$ and $\varpi \in C^m([a,T])$. Based on Ref. [28] and the definition of the ELRL integral, we find that the IVP (14) is equivalent to the following relation

$$\varpi(t) = \sum_{r=0}^{l-1} \frac{t^r}{r!}\varpi_0^{(r)} + \frac{1}{\Gamma_{Ext.}(q,\eta)} \int_a^t (t-y)^{q-1}\varpi(y,\varpi(y))dy \tag{15}$$

provided that the function w is continuous. Setting $\varepsilon = T/L, L \in Z^+, \varpi_k = k\varepsilon, k = 0,1,...,L,$ the solution of Eq. (15) is approximated, as given by Eq. (16), as follows

$$\varpi_\varepsilon(t_{k+1}) = \sum_{r=0}^{l-1} \frac{t_{k+1}^r}{r!}\varpi_0^{(r)} + \frac{\varepsilon^q}{\eta^2 \Gamma_{Ext.}(2+q,\eta)} \left[w\left(t_{k+1}, \varpi_\varepsilon^P(t_{k+1})\right) \right] + \sum_{i=0}^k v_{i,k+1} w(t_i, \varpi_\varepsilon(t_i)), \tag{16}$$

where $\varpi^P(t_{k+1})$ refers to the prediction value and

$$v_{i,k+1} = \begin{cases} k^{1+q} - (1+k)^q(k-q), \\ (k-i+2)^{1+q} + (k-i)^{1+q} - 2(k-i+1)^{1+q}, 1 \leq i \leq k, \\ 1, i = k+1, \end{cases} \tag{17}$$

$$\varpi_\varepsilon^P(t_{k+1}) = \sum_{r=0}^{l-1} \frac{t_{k+1}^r}{r!}\varpi_0^{(r)} + \frac{1}{\eta \Gamma_{Ext.}(1+q,\eta)} \sum_{i=0}^k \chi_{i,k+1} w(t_i, \varpi_\varepsilon(t_i)), \chi_{i,k+1} = \varepsilon^q[(k+1-i)^q - (k-i)^q].$$
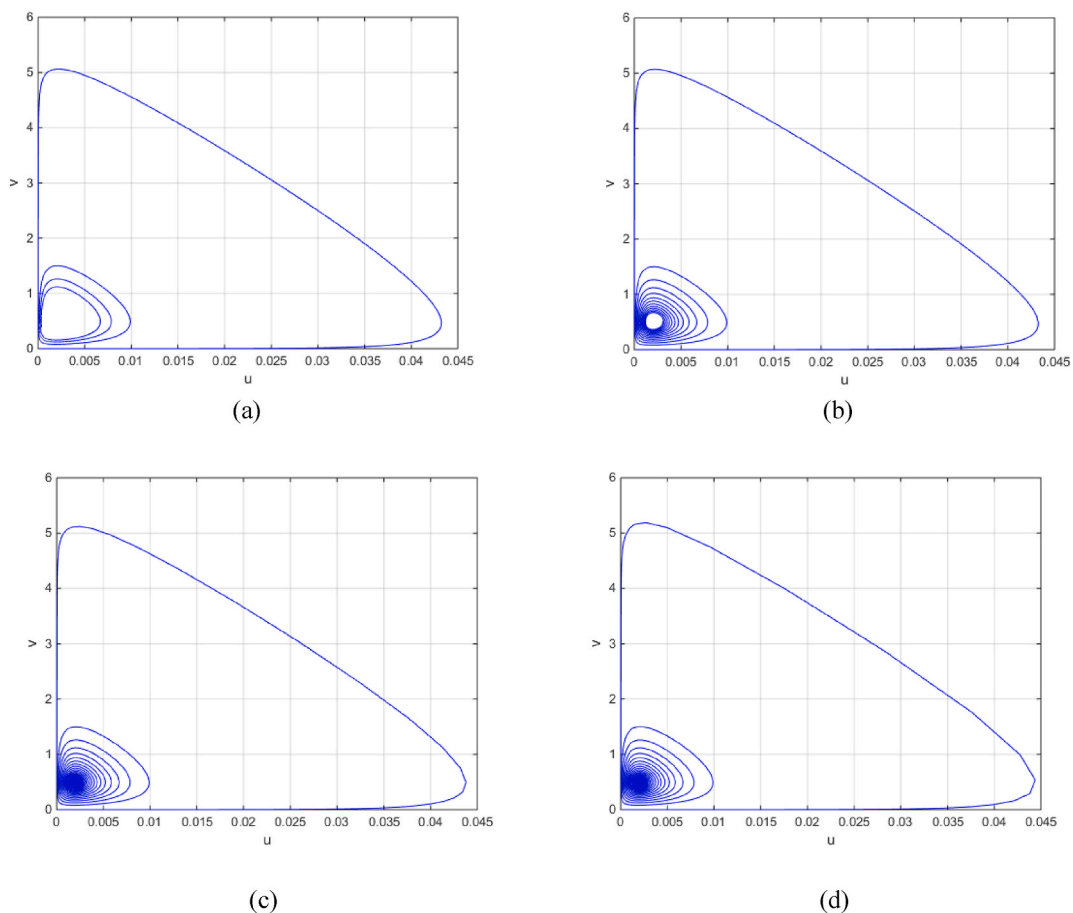

Fig. 1. The phase portraits of the AMR system (7) using the set A = $\{0.5, 100, 0.2\}, q = 0.99$ and (a) $\eta = 1$, (b) $\eta = 3$, (c) $\eta = 10$ and (d) $\eta = 15$.

The error of the modified scheme can be estimated via formula (18) that can be represented as

$$\max_{i=0,1,\ldots,L}|\boldsymbol{\varpi}(t_i) - \boldsymbol{\varpi}_e(t_i)| = O(\varepsilon^\rho), \tag{18}$$

in which $\rho = \min(1 + q, 2)$..

4.2. Numerical results

System (7) is numerically integrated based on the above-mentioned PECE scheme, in which we use the step size of $\mathbf{0.01}$, the ICs $\boldsymbol{u_0} = \mathbf{0.0002}, \boldsymbol{v_0} = \mathbf{0.0002}$, the parameter set $\mathbf{A} = \{\mathbf{0.5}, \mathbf{100}, \mathbf{0.2}\}$ and varying the fractional parameters $\boldsymbol{q}$ and $\boldsymbol{\eta}$. The numerical results, which are summarized in Fig. 1(a–d) and Fig. 2(a–d), show that the new fractional parameter $\boldsymbol{\eta}$ enables system (7) to exhibit various dynamical behaviors.

5. Complex dynamics in the discrete-time AMR system (13)

To check the existence of NS bifurcation in system (13) near the coexistence point $\mathbf{P_2}$, we use the parameter values $\boldsymbol{\alpha} = \mathbf{2}, \boldsymbol{\gamma} = \mathbf{0.3}$, $\boldsymbol{\mu}(\mathbf{0.85}, \mathbf{0.01}, \mathbf{5}) \approx \mathbf{0.0829}$ and the critical parameter $\boldsymbol{\beta_c} \approx \mathbf{12.3667}$. A limit cycle around the coexistence point $\mathbf{P_2}$ is illustrated in Fig. 3. The stability conditions of the NS bifurcation can be investigated as follows; we begin with considering a general form of system (13), with the bifurcation parameter $\boldsymbol{p}$, as described by Eq. (19)

$$\boldsymbol{\Upsilon_{n+1}} = \boldsymbol{f_p}(\boldsymbol{\Upsilon_n}). \tag{19}$$

The coexistence point $\mathbf{P_2} \neq (\mathbf{0,0})$, so with setting $(\boldsymbol{\Lambda}, \boldsymbol{p'}) = (\boldsymbol{\Upsilon} - \mathbf{P_2}, \boldsymbol{p} - \boldsymbol{p_c})$, we use the following transformation (20) as follows

$$\boldsymbol{\Lambda_{n+1}} = \boldsymbol{J}\Big((\mathbf{0,0}), \boldsymbol{p'}\Big)\boldsymbol{\Lambda_n} + \mathbf{0.5M}(\boldsymbol{\Lambda_n}, \boldsymbol{\Lambda_n}) + \frac{\mathbf{N}(\boldsymbol{\Lambda_n}, \boldsymbol{\Lambda_n}, \boldsymbol{\Lambda_n})}{\mathbf{6}} + \boldsymbol{O}\big(\|\boldsymbol{\Lambda_n}\|^4\big), \tag{20}$$
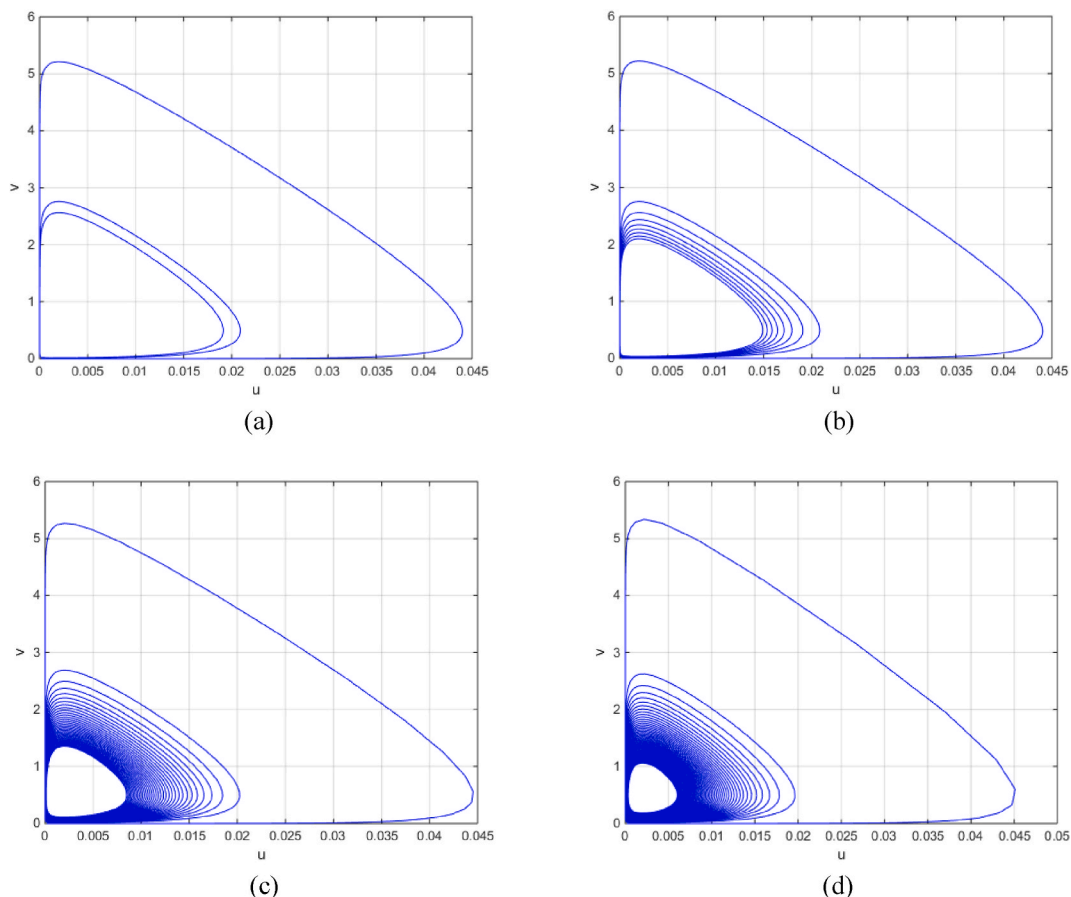

Fig. 2. The phase portraits of the AMR system (7) using the set A $= \{0.5, 100, 0.2\}, q = 0.9999$ and (a) $\eta = 1$, (b) $\eta = 3$, (c) $\eta = 10$ and (d) $\eta = 15$..
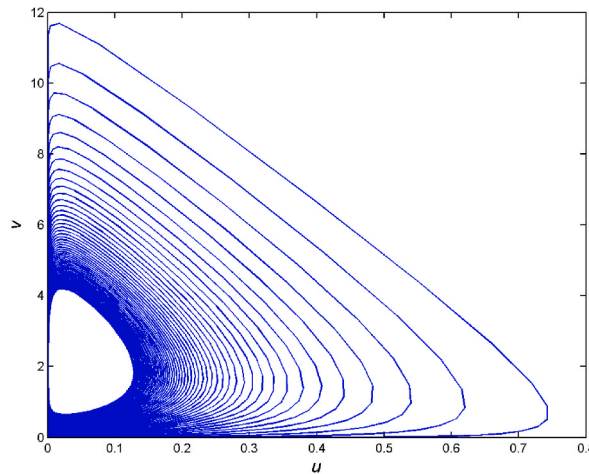
Fig. 3. The appearance of a stable limit cycle in system (13) when $\alpha = 2, \beta = 12.37, \gamma = 0.3$ and $\mu \approx 0.0829$.

$$\mathbf{M}_i(\boldsymbol{\rho}, \boldsymbol{\sigma}) = \sum_{s,k=1}^{n} \frac{\partial^2 \Lambda_i(\boldsymbol{\varepsilon})}{\partial \boldsymbol{\varepsilon}_s \partial \boldsymbol{\varepsilon}_k}\bigg|_{\varepsilon=0} \rho_j \sigma_k, \mathbf{N}_i(\boldsymbol{\rho}, \boldsymbol{\sigma}, \boldsymbol{\varsigma}) = \sum_{s,k,m=1}^{n} \frac{\partial^3 \Lambda_i(\boldsymbol{\varepsilon})}{\partial \boldsymbol{\varepsilon}_s \partial \boldsymbol{\varepsilon}_k \partial \boldsymbol{\varepsilon}_m}\bigg|_{\varepsilon=0} \rho_j \sigma_k \varsigma_m, i = 1, 2.$$

in addition, we obtain the following Jacobian defined by Eq. (21)

$$J(0,0) = \begin{pmatrix} 0.9959792253 & -0.002010387578 \\ 1.999999794 & 1 \end{pmatrix},\tag{21}$$

whose eigenvalues are given by $e^{\pm j\omega_c}$. The stability of the NS bifurcation can be checked by calculating the following quantity [29] that is defined by Eq. (22)

$$l_1(0) = 0.5\left[\operatorname{Re}\left(\delta_{21}e^{-j\omega_c}\right) - \operatorname{Re}\left(\delta_{20}\delta_{11}\frac{e^{-2j\omega_c} - 2e^{-j\omega_c}}{1 - e^{j\omega_c}}\right) - |\delta_{11}|^2 - 0.5|\delta_{02}|^2\right],\tag{22}$$

where

$$\delta_{20} = \langle\boldsymbol{\theta}, \mathbf{M}(\boldsymbol{\rho}, \boldsymbol{\rho})\rangle, \delta_{11} = \langle\boldsymbol{\theta}, \mathbf{M}(\boldsymbol{\rho}, \overline{\boldsymbol{\rho}})\rangle, \delta_{02} = \langle\boldsymbol{\theta}, \mathbf{M}(\overline{\boldsymbol{\rho}}, \overline{\boldsymbol{\rho}})\rangle,$$

$$\delta_{21} = \langle\boldsymbol{\theta}, \mathbf{N}(\boldsymbol{\rho}, \boldsymbol{\rho}, \overline{\boldsymbol{\rho}})\rangle + 2\langle\boldsymbol{\theta}, \mathbf{M}(\boldsymbol{\rho}, (diag(1,1) - J)^{-1}\mathbf{M}(\boldsymbol{\rho}, \overline{\boldsymbol{\rho}}))\rangle + \langle\boldsymbol{\theta}, \mathbf{M}(\overline{\boldsymbol{\rho}}, (e^{2j\omega_c}diag(1,1) - J)^{-1}\mathbf{M}(\boldsymbol{\rho}, \boldsymbol{\rho}))\rangle - \frac{2 - e^{-j\omega_c}}{1 - e^{j\omega_c}}\delta_{20}\delta_{11}$$

$$- \frac{2}{1 - e^{-j\omega_c}}|\delta_{11}|^2 - \frac{e^{j\omega_c}}{e^{3j\omega_c} - 1}|\delta_{02}|^2,$$

in which the vectors $\boldsymbol{\theta}$ and $\boldsymbol{\rho}$ must satisfy the relations (23)

$$J(p')\rho = e^{j\omega_c}\rho, J(p')\overline{\rho} = e^{-j\omega_c}\overline{\rho}, J^T(p')\theta = e^{-j\omega_c}\theta, J^T(p')\overline{\theta} = e^{j\omega_c}\overline{\theta}, \langle\boldsymbol{\theta}, \boldsymbol{\rho}\rangle = 1.\tag{23}$$

So, the numerical values of $\boldsymbol{\theta}$ and $\boldsymbol{\rho}$ are obtained via equation (24) as follows

$$\begin{aligned}\rho &= (-0.03168885416 - 0.001005193804j, j)^T,\\ \theta &= (-11.09733262 + 2.236120619j, -0.08201507022 + 0.6505859797j)^T.\end{aligned}\tag{24}$$

Moreover, we obtain the matrices defined by equation (25) as follows

$$\mathbf{M}(\boldsymbol{\rho}, \boldsymbol{\sigma}) = \begin{pmatrix} -\mu(2\alpha\rho_1\sigma_1 + \rho_1\sigma_2 + \rho_2\sigma_1) \\ \mu\beta(\rho_1\sigma_2 + \rho_2\sigma_1) \end{pmatrix}, \mathbf{N}(\boldsymbol{\rho}, \boldsymbol{\sigma}, \boldsymbol{\varsigma}) = \begin{pmatrix} 0 \\ 0 \end{pmatrix},\tag{25}$$

The following quantities defined in Eq. (26) are straightforwardly obtained

$$\begin{aligned}\delta_{20} &= -0.02518999422 - 0.05294915055j,\\ \delta_{11} &= 0.002017868406 + 0.001712999489j,\\ \delta_{02} &= 0.03593048476 + 0.05250057217j,\\ \delta_{21} &= -0.00479011521 - 0.01082334344j,\end{aligned}\tag{26}$$

which imply that $l_1(0) = -0.00255 < 0$. Hence, the NS bifurcation around the coexistence point $\mathbf{P}_2$ is stable.

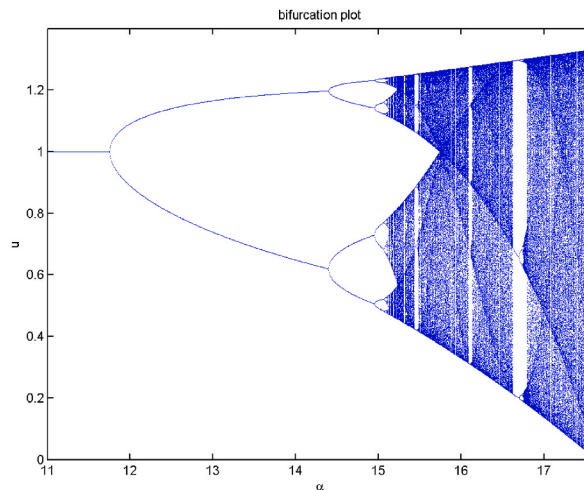**Fig. 4.** A bifurcation diagram of system (13), showing flip bifurcation when $\beta = 0.5, \gamma = 1, \mu = 0.1701654293$ and varying α..

Then, we study the conditions of flip bifurcation in system (13). It is clear that the axial equilibrium point $\mathbf{P_1}$ exhibits flip bifurcation when $\beta = 0.5, \gamma = 1, \mu(0.8, 0.01, 10) = 0.1701654293$ and $\alpha_c = 11.75326862$..

To discuss the stability of flip bifurcation, we firstly use the matrices defined in Eq. (20) using the critical value α_c and

$$\begin{aligned}\boldsymbol{\rho} &= (\mathbf{1}, \mathbf{0})^T, \\ \boldsymbol{\theta} &= (\mathbf{1}, \mathbf{0.4319})^T.\end{aligned} \tag{27}$$

The stability of the flip bifurcation can be checked by calculating the following quantity [29], which is defined by Eq. (28)

$$\boldsymbol{\Omega}(\mathbf{0}) = \frac{\langle \boldsymbol{\theta}, \mathbf{N}(\boldsymbol{\rho}, \boldsymbol{\rho}, \boldsymbol{\rho}) \rangle}{6} - \frac{\langle \boldsymbol{\theta}, M(\boldsymbol{\rho}, (\boldsymbol{J} - \boldsymbol{diag}(\mathbf{1}, \mathbf{1}))^{-1} \mathbf{M}(\boldsymbol{\rho}, \boldsymbol{\rho})) \rangle}{2}. \tag{28}$$

Here, it is found that (See Eq. (29))

$$M(\rho, (\boldsymbol{J} - \boldsymbol{diag}(\mathbf{1}, \mathbf{1}))^{-1} \mathbf{M}(\rho, \boldsymbol{\rho})) = -2(\alpha^2 \mu^2, 0)^T, \tag{29}$$

which implies that $\boldsymbol{\Omega}(\mathbf{0}) = \alpha^2 \mu^2 > 0$. Hence, the bifurcating period 2 orbits around the axial equilibrium point $\mathbf{P_1}$ are stable. Fig. 4 gives the bifurcation diagram that illustrates this interesting bifurcation phenomenon.

Finally, rich complex dynamics in system (13) are observed when the ICs are selected as $\boldsymbol{u_0} = \mathbf{1.01}, \boldsymbol{v_0} = \mathbf{0.01}$, and the parameters are fixed at $\beta = 3.2, \gamma = 1, q = 0.1, m = 0.01, \eta = 2/3$ and varying α. The results are illustrated in Fig. 5(a–e), in which the CIC, the strange attractors with fractal or multi-fractal structures, the coexistence of multi-strange attractors, and the existence of chaotic attractors are shown.

6. Complex dynamics in the AMR system using the EFFO-C

Here, we will discuss the complex dynamics in the AMR system using the EFFO-C, which is given by equation (5). The resulting system is described as

$$\begin{aligned}{}^{EFF}_{C}\mathbf{O}^{q,p,\eta}_{0,t}(\boldsymbol{u}(t)) &= \alpha u(1 - u) - uv, \\ {}^{EFF}_{C}\mathbf{O}^{q,p,\eta}_{0,t}(\boldsymbol{v}(t)) &= \beta uv - \gamma v.\end{aligned} \tag{30}$$

The results of numerical integration for system (30) are depicted in Fig. 6(a–d) and Fig. 7(a–d).

Obviously, the results illustrated by Figs. 6 and 7 are similar to the results illustrated by Figs. 1 and 2, respectively. Hence, modeling the complex dynamics in this system can adequately be estimated using these types of equivalent fractional operators. Moreover, the extended fractal-fractional operator is a better candidate to display more complex dynamics since it has a higher degree of freedom.

7. Conclusion

The ELCFDO and ERCFDO have been introduced. Some basic features of the new fractional differential operators and the new fractional integrals have been presented in the form of new mathematical lemmas in order to provide detailed and rigorous theoretical derivations that can support the application of the generalized Gamma function to the extended fractional operators. All the new lemmas have been proven.

The fractional AMR model has been investigated using the ELCFDO. The relevance between the fractional operators and the AMR
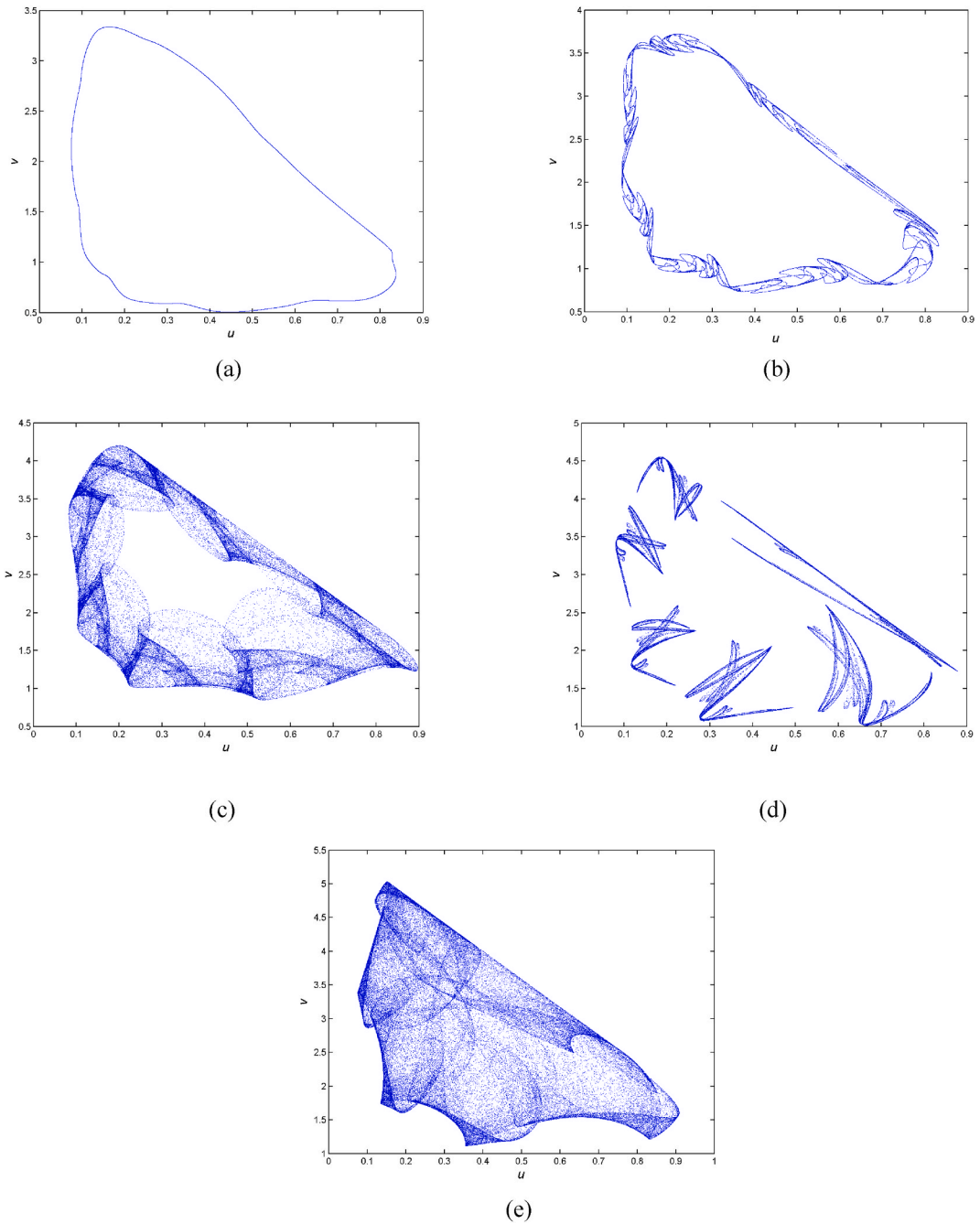
Fig. 5. The phase portraits of system (13) using $\beta = 3.2, \gamma = 1, q = 0.1, m = 0.01, \eta = 2/3$ showing: (a) CIC for $\alpha = 3$, (b) continuous merging of strange attractors for $\alpha = 3.6$, (c) a merged chaotic attractor for $\alpha = 4.1$, (d) coexistence of multi-strange attractors for $\alpha = 4.5$, and (e) a chaotic attractor for $\alpha = 5$..
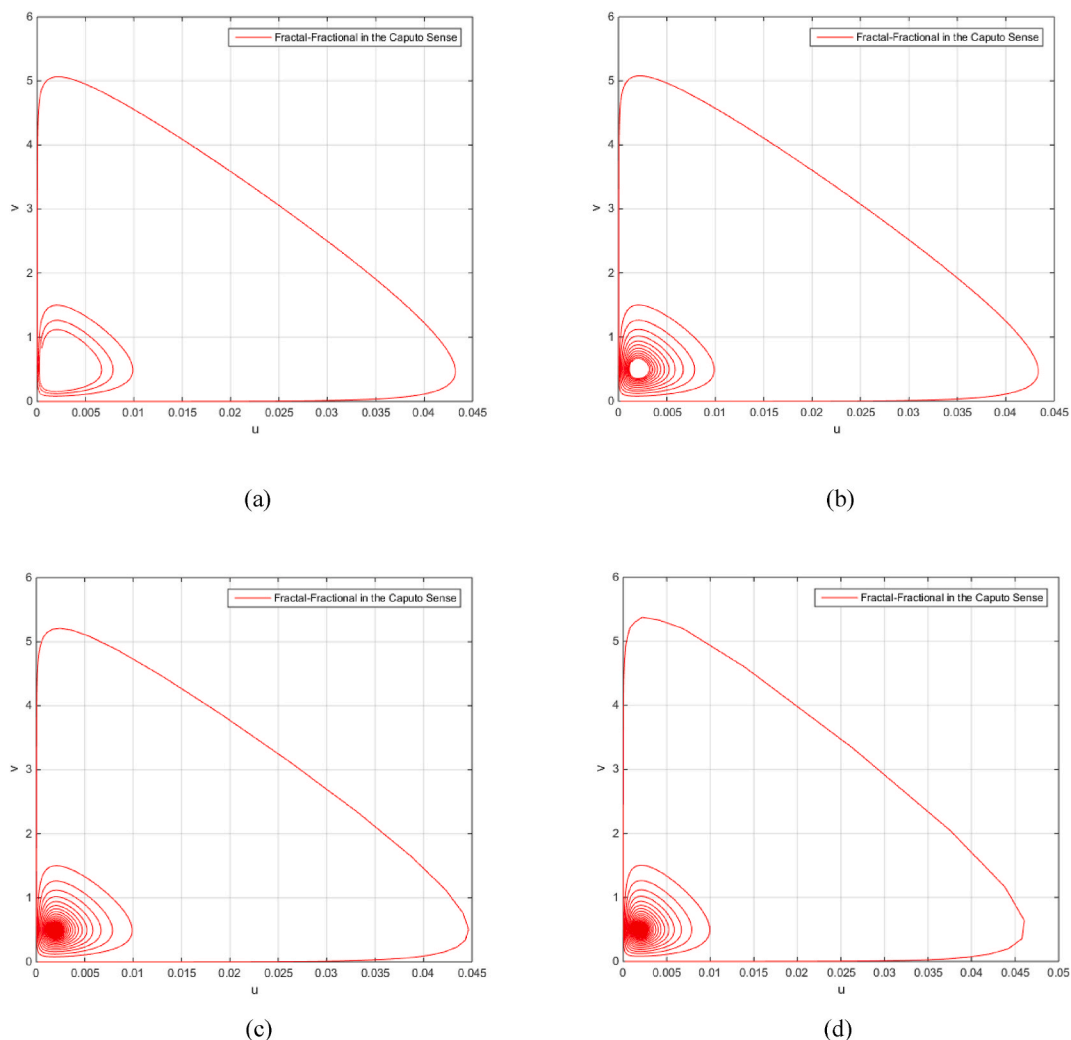
(a)

(b)

(c)

(d)

Fig. 6. The phase portraits of the AMR system (30) using the set $\mathbf{A} = \{0.5, 100, 0.2\}, q = 0.99, p = 0.99$ and (a) $\eta = 1$, (b) $\eta = 3$, (c) $\eta = 10$ and (d) $\eta = 15..$

model has also been discussed to enhance the credibility and validity of such a model. To numerically integrate the proposed fractional system using the ELCFDO, a modification to the PECE algorithm has been explained. It has been found that the new parameter of the ELCFDO enables the AMR system to exhibit a variety of complex dynamics. Furthermore, the discretization of the ELCFDO has been obtained using piecewise constant arguments. Then, a variety of complex dynamics in the discrete-time version of the fractional AMR system involving the ELCFDO have been obtained such as the existence of the NS bifurcation and the period-doubling bifurcation, the existence of CIC, the existence of strange attractors with fractal or multi-fractal structures, and chaotic attractors.

On the other hand, the EFFO-C has been introduced based on the generalized Gamma function. Then, the EFFO-C is also applied to the AMR system, which displays complex dynamics that are similar to those in the case of the corresponding ELCFDO. Thus, the two new extended fractional operators display similar dynamic phenomena when applied in this system with a specific choice of parameter values. In addition, the EFFO-C has a higher degree of freedom that makes the system able to display more complex dynamics.

Throughout this work, many comparisons have been carried out between the results obtained using the generalized Gamma function and other established numerical methods for solving fractional-order systems. The results of such comparisons assert that the proposed new fractional operators are better candidates to handle the complex dynamics of the AMR model.

This work can be extended in future studies to investigate the higher dimensional AMR systems involving the ELCFDO or the ERCFDO. In addition, this kind of study provides higher adequacy and a better understanding of the model's complex dynamics, which can help to estimate and predict the spread of diseases that appear due to antimicrobial-resisting bacteria. Furthermore, all the proposed operators can be applied to many systems arising from different disciplines in order to obtain a more precise description of the models' natural phenomena.
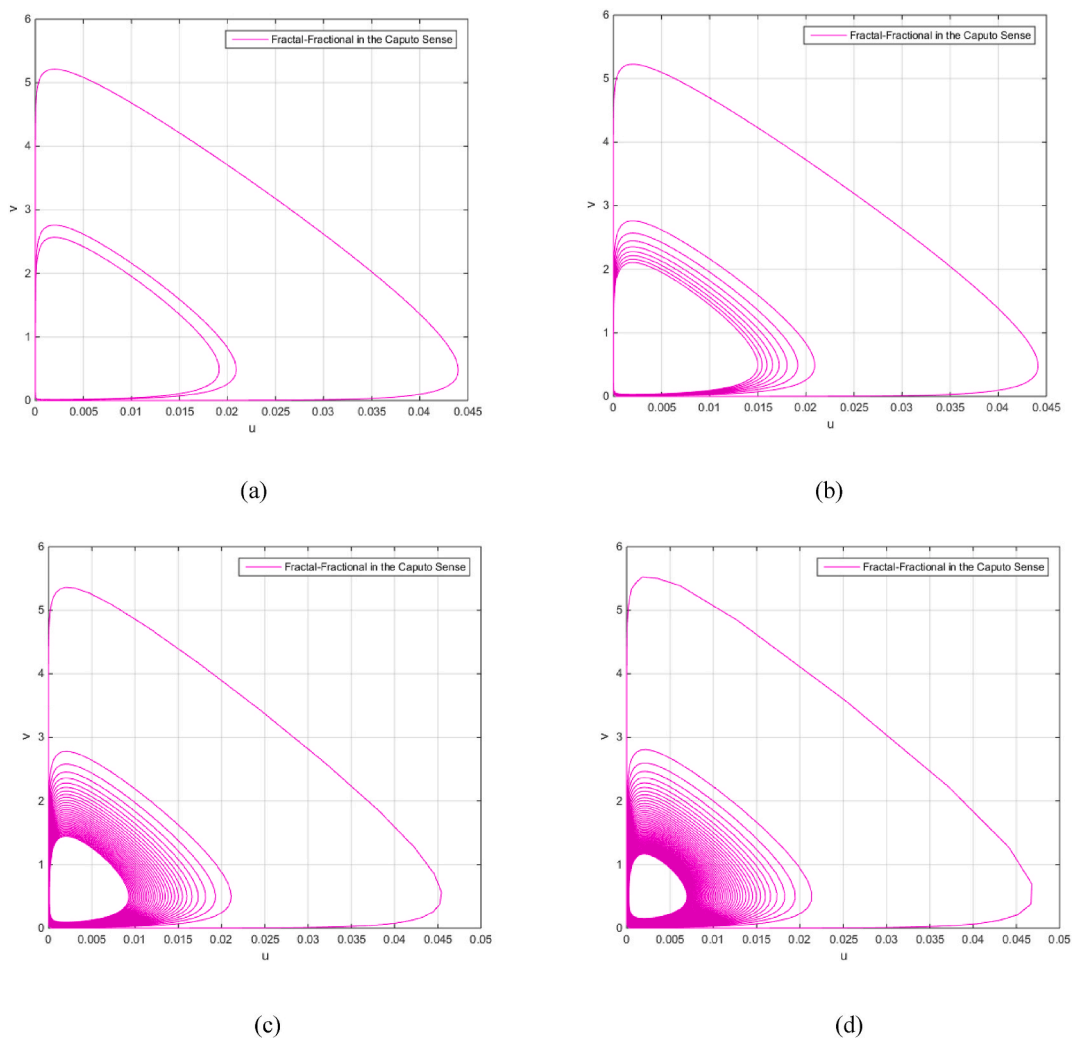
Fig. 7. The phase portraits of the AMR system (30) using the set $A = \{0.5, 100, 0.2\}, q = 0.9999, p = 0.99$ and (a) $\eta = 1$, (b) $\eta = 3$, (c) $\eta = 10$ and (d) $\eta = 15$..

Author contribution statement

Data availability statement

No data was used for the research described in the article.

Additional information

No additional information is available for this paper.

Declaration of competing interest

The authors declare that they have no known competing financial interests or personal relationships that could have appeared to influence the work reported in this paper.

Acknowledgement

References

[1] A. Shahzad, et al., Brownian motion and thermophoretic diffusion impact on Darcy-Forchheimer flow of bioconvective micropolar nanofluid between double disks with Cattaneo-Christov heat flux, Alex. Eng. J. 62 (2023) 1–15.

[2] F.K. Iyanda, H. Rezazadeh, M. Inc, A. Akgül, I.M. Bashiru, M.B. Hafeez, M. Krawczuk, Numerical simulation of temperature distribution of heat flow on reservoir tanks connected in a series, Alex. Eng. J. 66 (2023) 785–795.

[3] K. Abuasbeh, S. Qureshi, A. Soomro, An Optimal family of block techniques to solve models of infectious diseases: fixed and adaptive stepsize strategies, Mathematics 11 (5) (2023) 1135.

[4] M.S. Iqbal, M.W. Yasin, N. Ahmed, A. Akgül, M. Rafiq, A. Raza, Numerical simulations of nonlinear stochastic Newell-Whitehead-Segel equation and its measurable properties, J. Comput. Appl. Math. 418 (2023), 114618.

[5] M.I. Liaqat, A. Akgül, M.D. Sen, M. Bayram, Approximate and exact solutions in the sense of conformable derivatives of quantum mechanics models using a novel algorithm, Symmetry 15 (2023) 744.

[6] A. Hasan, A. Akgül, M. Farman, F. Chaudhry, M. Sultan, M.D. Sen, Epidemiological analysis of symmetry in transmission of the Ebola virus with power law kernel, Symmetry 15 (2023) 665.

[7] M. Qayyum, E. Ahmad, S.T. Saeed, A. Akgül, M.B. Riaz, Traveling wave solutions of generalized seventh- order time-fractional KdV models through He-Laplace algorithm, Alex. Eng. J. 70 (2023) 1–11.

[8] M. Awadalla, S. Qureshi, A. Soomro, K. Abuasbeh, A Novel three-step numerical solver for physical models under fractal behaviour, Symmetry 15 (2023) 330.

[9] A.E. Matouk, Stability conditions, hyperchaos and control in a novel fractional order hyperchaotic system, Phys. Lett. 373 (2009) 2166–2173.

[10] A.E. Matouk (Ed.), Advanced Applications of Fractional Differential Operators to Science and Technology, IGI Global, Hershey PA, USA, 2020.

[11] A. Kumar, S.S. Alzaid, B.S.T. Alkhatani, S. Kumar, Complex dynamic behaviour of food web model with generalized fractional operator, Mathematics 10 (2022) 1702.

[12] A. Zenkour, A. Abouelregal, Fractional thermoelasticity model of a 2D problem of mode-I crack in a fibre-reinforced thermal environment, J. Appl. Comput. Mech. 5 (2019) 269–280.

[13] A. Abouelregal, H. Ahmad, A modified thermoelastic fractional heat conduction model with a single lag and two different fractional orders, J. Appl. Comput. Mech. 7 (2021) 1676–1686.

[14] S. Westerlund, Dead Matter Has Memory! Kalmar, , Causal Consulting, Sweden, 2002.

[15] M. Zhang, W. Weng, Z. Yan, Interactions of fractional N-solitons with anomalous dispersions for the integrable combined fractional higher-order mKdV hierarchy, Phys. Nonlinear Phenom. 444 (2023), 133614.

[16] A.E. Matouk, Chaotic attractors that exist only in fractional-order case, J. Adv. Res. 45 (2023) 183–192.

[17] N. Laskin, Fractional market dynamics, Physica A 287 (2000) 482–492.

[18] A. Padder, L. Almutairi, S. Qureshi, A. Soomro, A. Afroz, E. Hincal, A. Tassaddiq, Dynamical analysis of generalized tumor model with Caputo fractional-order derivative, Fractal and Fractional 7 (3) (2023) 258.

[19] S. Qureshi, Z. Memon, Use of real data application for analysis of the measles disease under Caputo-Fabrizio-Caputo operator, in: Applications of Fractional Calculus to Modeling in Dynamics and Chaos, Chapman and Hall/CRC, 2022, pp. 379–406.

[20] R. Jan, S. Qureshi, S. Boulaaras, V.-T. Pham, E. Hincal, R. Guefaifia, Optimization of the Fractional-Order Parameter with the Error Analysis for Human Immunodeficiency Virus under Caputo Operator, Discrete and Continuous Dynamical Systems-S, 2023, https://doi.org/10.3934/dcdss.2023010.

[21] M. Caputo, Linear models of dissipation whose Q is almost frequency independent-II, Geophys. J. R. Astron. Soc. 13 (1967) 529–539.

[22] A. Atangana, Fractal-fractional differentiation and integration: connecting fractal calculus and fractional calculus to predict complex system, Chaos Solit. Fract. 102 (2017) 396–406.

[23] S.K. Agarwal, S.L. Kalla, A generalized gamma distribution and its application in reliability, Commun. Statist. Theory Meth. 25 (1996) 201–210.

[24] E. Ahmed, A.E. Matouk, Complex dynamics of some models of antimicrobial resistance on complex networks, Math. Meth. Appl. Sci. 44 (2021) 1896–1912.

[25] A. Kilbas, H.M. Srivastava, J.J. Trujillo, Theory and Applications of Fractional Differential Equations, North-Holland Mathematics Studies, Elsevier Science B. V. Amsterdam, 2006, 204.

[26] A.M.A. El-Sayed, F.M. Gaafar, H.H.G. Hashem, On the maximal and minimal solutions of arbitrary orders nonlinear functional integral and differential equations, Math. Sci. Res. J. 8 (11) (2004) 336–348.

[27] K. Diethelm, N.J. Ford, A.D. Freed, A predictor–corrector approach for the numerical solution of fractional differential equations, Nonlinear Dyn 29 (2002) 3–22.

[28] K. Diethelm, N.J. Ford, Analysis of fractional differential equations, J. Math. Anal. Appl. 265 (2002) 229–248.

[29] Y.A. Kuznetsov, Elements of Applied Bifurcation Theory, second ed., Springer-Verlag, New York, 1998.